

# Optical responses of the switching currents in Al and Nb Josephson junctions

Yiwen Wang,<sup>1</sup> Pinjia Zhou,<sup>1</sup> Lianfu Wei,<sup>1,2, a)</sup> Beihong Zhang,<sup>1</sup> Qiang Wei,<sup>1</sup> Jiquan Zhai,<sup>3</sup> Weiwei Xu,<sup>3</sup> and Chunhai Cao<sup>3</sup>

<sup>1)</sup>Quantum Optoelectronics Laboratory, School of Physics, Southwest Jiaotong University, Chengdu 610031, China

<sup>2)</sup>State Key Laboratory of Optoelectronic Materials and Technologies, School of Physics and Engineering, Sun Yat-Sen University, Guangzhou 510275, China

<sup>3)</sup>Research Institute of Superconductor Electronics, Department of Electronic Science and Engineering, Nanjing University, Nanjing 210093, China

We experimentally demonstrated the optical responses of the switching currents in two types of Josephson tunnel junctions: Al/AlOx/Al and Nb/AlOx/Nb. The radiation-induced switching current shifts were measured at ultra-low bath temperature ( $T \approx 16$  mK). It is observed that the Al-junction has a more sensitive optical response than the Nb-junction, which is as expected since Al electrode has a smaller superconducting gap energy. The minimum detectable radiation powers with the present Al-junction and Nb-junction are 8 pW (corresponding to  $8 \times 10^5$  incoming photons in one measurement cycle) and 2 nW respectively. In addition, we found that the radiation-induced thermal effects are dominant in the observed optical responses. Several methods are proposed to further improve the optical responsivity, so that the Josephson junction based devices could be applicable in photon detections.

Superconducting photon detectors at near-infrared wavelengths, with photon-number resolving power, have shown great promises in quantum optics and quantum information applications. The superconducting detectors mainly include superconducting nanowire detectors (SNSPDs)<sup>1-4</sup>, transition-edge sensors (TESs)<sup>5,6</sup>, superconducting tunnel junctions (STJs)<sup>7,8</sup> and microwave kinetic inductance detectors (MKIDs)<sup>9-11</sup>, etc.. Actually, photon detections can also be achieved through other ways, such as by measuring the changes in the critical current of a Josephson tunnel junction due to radiation. Physically, a photon with sufficient energy  $h\nu$  ( $> 2\Delta$ ) can directly break  $\eta h\nu/2\Delta$  Cooper pairs, where  $\Delta$  is the superconducting gap energy and  $\eta$  the convert efficiency. Therefore, when a photon is incident on one superconducting electrode of the Josephson junction, excess quasiparticles will be excited and the Cooper pair density on the irradiated electrode will decrease. This will lead to an abrupt reduction in the critical current  $I_c$  since<sup>12</sup>  $I_c \propto \sqrt{\rho_1 \rho_2}$ , where  $\rho_i$  is the Cooper pair density on the  $i$ -th electrode. On the other hand, phonons in the substrate around the radiation center may be excited and thus cause a temperature increase nearby the junction area. This thermal effect can also reduce the critical current  $I_c$  based on the relation<sup>13</sup>

$$I_c R_n = [\pi \Delta(T)/2e] \tanh[\Delta(T)/2k_B T], \quad (1)$$

with  $R_n$  being the normal state resistance and  $T$  the bath temperature. Since the gap energy  $\Delta(T)$  decreases with  $T$ , the critical current  $I_c$  also decreases with  $T$ . Therefore, both pure pair-breaking effects and thermal effects can lead to a reduction in the critical current. This provides a feasible way to detect the incident photons via measuring the radiation-induced changes in the critical current of a Josephson junction.

Note that the well-known *ac* Josephson effect was utilized to detect the microwave and far-infrared radiation several years ago<sup>14</sup>. Later, the superconducting gap voltage shifts due to visible and infrared radiation were measured in Nb/AlOx/Nb junctions<sup>15</sup> and junction arrays<sup>16</sup> at temperatures around 4.2 K. Specifically, the junctions immersed in superfluid helium were observed to have lower optical responsivity compared to those in vacuum. This is because the heating effect is suppressed in liquid helium and thus the optical responses of the devices are entirely due to the pair-breaking mechanism. Other experiments<sup>17-20</sup> with Nb junctions had also verified these responses due to pure pair-breaking and thermal effects.

However, the previous experiments were all done with Nb junctions. In our experiments, we studied the optical responses of both Al- and Nb junctions. We found that the Al-junction has a more sensitive optical response than Nb-junction. This is a reasonable observation since aluminum has a smaller gap energy. Thus, a certain radiation energy can break more Cooper pairs on Al electrode. Besides, in all of the previous experiments the Josephson junctions were biased at constant currents and the gap voltage shifts were measured as the optical responses. Alternatively, we swept the bias current through the junction and measured the switching current responses to a continuous radiation at 1550 nm. This detection approach is relatively simple and has not been reported before, as far as we know. Moreover, the previous experiments were all done at temperatures around 1 K  $\sim$  4.2 K while our system works in an ultra-low temperature regime, i.e., the bath temperature  $T \approx 16$  mK. Thermal noise in the circuit is minimized at such low temperatures and thus devices are expected to have more sensitive optical responses.

For our measurements, the Al/AlOx/Al junction was fabricated by electron beam double-angle evaporation, and the Nb/AlOx/Nb junction was fabricated by magnetron sputtering and ion etching. For both Al and Nb

<sup>a)</sup>Electronic mail: weilianfu@gmail.com

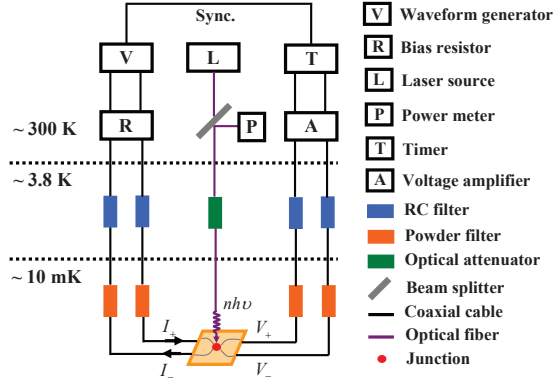


FIG. 1. (Color online) Schematics of the measurement setup. Four-probe method is used to measure the junction current-voltage characteristics. The tested junction is placed in the sample cell at  $\sim 16$  mK and irradiated by 1550 nm laser beam.

devices, the junction areas are about  $6 \mu\text{m}^2$  and the top electrodes exposed for illumination are about 100 nm thick. The chips are cut to approximately  $2 \text{ mm} \times 2 \text{ mm}$ , with Si-substrates of 0.5 mm thick. Both junctions are slightly damped<sup>21</sup> and show hysteretic IV curves with small retrapping currents and sharp onsets of voltage at the maximum bias currents (i.e., the switching currents).

The schematics of our measurement setup are shown in Fig. 1. The measured junction is placed in a superconducting aluminum sample cell, mounted at the mixing chamber in a dilution refrigerator with base temperature around 10 mK. Four-probe technique is used to measure the current-voltage characteristics of the devices. The waveform generator can output a voltage signal, which is applied to a resistor to generate a bias current through the junction. The voltage response is amplified by a battery-powered pre-amplifier and then fed into a timer. All electrical leads, connecting the sample cell to room temperature electronics, are filtered by low-pass RC filters and copper powder microwave filters. To radiate the junction, a single-mode optical fiber is set up from the room temperature environment down to the sample cell. A laser source is connected to the top end of the fiber and generates a steady radiation of wavelength 1550 nm. The bottom end of the fiber is carefully aligned and fixed, so that the laser beam can focus on the top electrode of the junction. The fiber end is estimated to be about  $200 \mu\text{m}$  vertically away from the chip surface and the irradiated area is about  $80 \mu\text{m}$  in diameter. Therefore, the junction area is completely covered by light.

Due to the presence of thermal fluctuations and quantum tunneling, the junction switches from the zero-voltage state to the finite voltage state at a bias current  $I_s$  smaller than its critical current  $I_c$ . Since this switching is a deterministic random process, the switching current  $I_s$  shows a Lorentzian distribution<sup>22,23</sup>, which can be mainly characterized by the width  $\sigma_s$  and mean

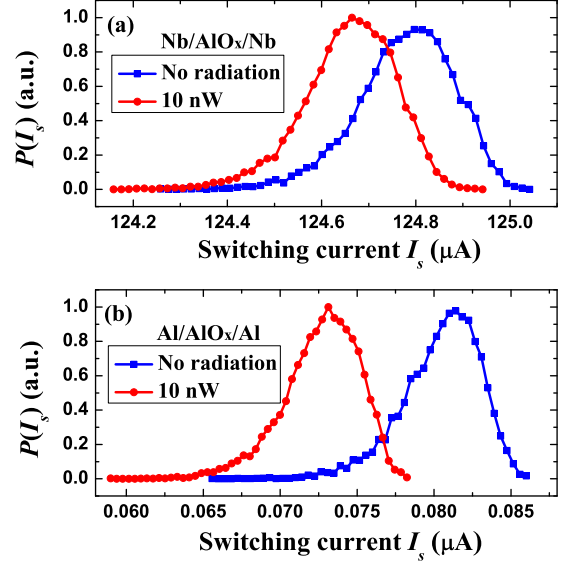


FIG. 2. (Color online) (a) The measured distributions of the switching currents of Nb/AlOx/Nb. Blue squares correspond to the data in the absence of radiation and red dots correspond to a 10 nW radiation on the junction. (b) The switching current distributions of Al/AlOx/Al without radiation and with a 10 nW radiation respectively.

value  $\langle I_s \rangle$ . In our experiment the switching current distribution  $P(I_s)$  is measured by using the time-of-flight method<sup>24</sup>. For each switching event, the bias current is ramped linearly from a value below zero up to a value higher than the critical current  $I_c$ . When the junction switches from the zero-voltage state to the finite-voltage state, the timer will be triggered to record the switching time and the corresponding switching current  $I_s$  can be calculated from the ramping rate. The bias current is then reduced to below zero, resetting the junction to the zero-voltage state. The repetition frequency is 71.3 Hz and the measurement cycle is repeated  $2 \times 10^3$  times to obtain an ensemble of  $I_s$ , from which the distribution of switching current  $P(I_s)$  can be obtained.

Fig. 2 plots the measured switching current distribution, i.e., the switching probability  $P(I_s)$  as a function of the switching current  $I_s$ . Fig. 2(a) shows the switching current measurements on Nb/AlOx/Nb at temperature 16 mK. The blue curve is the distribution in the absence of radiation, from which one can calculate the mean switching current  $\langle I_{s0}(\text{Nb}) \rangle = 124.78 \mu\text{A}$  and the distribution width (standard deviation)  $\sigma_{s0}(\text{Nb}) = 102.73 \text{ nA}$ . The red curve corresponds to a 10 nW radiation on the junction electrode. In this case the mean switching current shifts down to  $\langle I_s(\text{Nb}) \rangle = 124.66 \mu\text{A}$  and the distribution width  $\sigma_s(\text{Nb}) = 98.00 \text{ nA}$ . Fig. 2(b) shows the same measurements on Al/AlOx/Al under the same experimental conditions. Without radiation, the mean switching current is  $\langle I_{s0}(\text{Al}) \rangle = 80.44 \text{ nA}$  and the distribution width  $\sigma_{s0}(\text{Al}) = 2.53 \text{ nA}$ . In the presence of 10

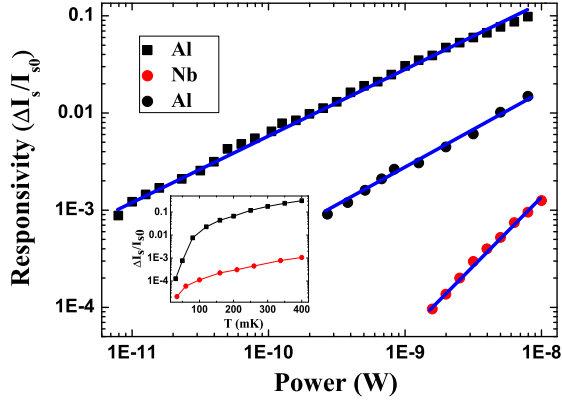


FIG. 3. (Color online) The logarithmic  $\Delta I_s/I_{s0}$  as a function of logarithmic radiation power. Black squares and black circles are the experimental data for focusing the light on junction and nearby substrate of Al device respectively. Red circles correspond to radiation on the junction of Nb device. The blue lines are the linear fitting, from which one can obtain the power law dependence of the responsivity. The inset shows  $\Delta I_s/I_{s0}$  as a function of the bath temperature.

nW radiation, the mean switching current is  $\langle I_{s1}(Al) \rangle = 72.65$  nA and the distribution width  $\sigma_{s1}(Al) = 2.47$  nA.

There are two ways to define the photon responsivity of the device. One is the ratio of the response to noise, i.e.,  $R_a = \Delta I_s/\sigma_{s0} = (\langle I_{s0} \rangle - \langle I_{s1} \rangle)/\sigma_{s0}$ . By this way, we have  $R_a = 1.17$  for the Nb-junction and  $R_a = 3.08$  for the Al-junction, showing that the Al device has a higher photon responsivity. The second way to define photon responsivity is the relative shift of switching current, i.e.,  $R_b = \Delta I_s/I_{s0} = (\langle I_{s0} \rangle - \langle I_{s1} \rangle)/\langle I_{s0} \rangle$ . In this way, we obtain  $R_b = 9.6 \times 10^{-4}$  for the Nb-junction and  $R_b = 9.7 \times 10^{-2}$  for the Al-junction, showing again that the Al device has a more sensitive response. We take the second definition of responsivity in the following discussions.

We now investigate the optical responses of the switching currents under different radiation powers. To this aim we varied the light intensity and measured the corresponding average switching current at the base temperature  $T = 16$  mK. Fig. 3 shows the relative switching current shift  $\Delta I_s/I_{s0}$  (i.e., the responsivity  $R_b$ ) as a function of the radiation power. The black squares and red circles correspond to irradiations on Al- and Nb-junction respectively. It is shown that the logarithmic switching current shift increases linearly with the logarithmic radiation power in the applied power range. By fitting the line slope, one can find that  $R_b$  is approximately proportional to  $P^{0.6}$  for the Al-junction while proportional to  $P^{1.2}$  for the Nb-junction. The minimum radiation power that the Al device can detect is about 8 pW (corresponding to  $8 \times 10^5$  incoming photons per measurement cycle), which is much smaller than the minimum power of 2 nW that Nb device can detect. The device response to low radiation power is limited by the average switching current fluctuations, which are mainly due to the inevitable

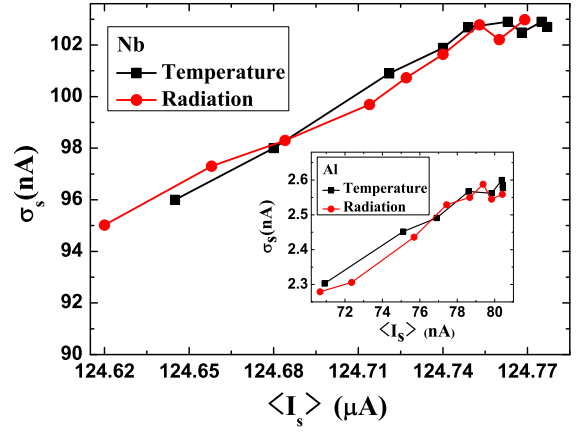


FIG. 4. (Color online) The list plots of the measured distribution width  $\sigma_s$  versus the average switching current  $\langle I_s \rangle$ , for the Nb-junction, due to independent changes in bath temperatures (black squares) and radiation powers (red circles) respectively. The inset shows the same plots for the Al-junction.

low-frequency noises in the electronics.

The switching current shift increases with the radiation power, which is qualitatively similar to its bath temperature dependence. The inset of Fig. 3 shows  $\Delta I_s/I_{s0}$  as a function of the bath temperature in the range of 30 mK to 400 mK, where the measured switching current shift increases with temperature. This suggests that the thermal effects are dominant in the observed radiation power dependence of  $R_b$  at  $T = 16$  mK. Experimentally, most of the photons are incident on the substrate rather than the superconducting electrode. Thus, the chip will be mainly heated and achieve an effective temperature greater than the bath temperature, since we are continuously pumping energy into the system. To verify that the thermal effects dominate the radiation power dependence of switching current, we moved the fiber to radiate directly on a small area of the bare substrate, which is about 0.7 mm away from the junction area. We then performed the same switching current measurements at 16 mK and obtained the radiation power dependence of  $R_b$ , shown in Fig. 3 (black circles). It is shown that the photon responsivity is apparently weaker, when radiating on the bare substrate of a certain distance away from the junction than that when focusing on the junction area. This is a reasonable result, which can be attributed to a nonuniform temperature distribution around the irradiated area. The effective temperature at the junction area is lower when the light spot is moved 0.7 mm away. The  $R_b$  exhibits the same radiation power law dependence (the same slope) for both cases of radiation on the junction and the substrate, indicating that the thermal effect is the main factor in shifting the switching current.

Furthermore, we measured the variations of the switching current distribution due to the changes in bath temperature and radiation power independently. Fig. 4 plots

the distribution width  $\sigma_s$  as a function of the average switching current  $\langle I_s \rangle$  for the Nb device. Here, the black squares correspond to the data at different bath temperatures and without radiation, while the red circles correspond to different radiation powers and at the lowest bath temperature. The inset shows the same plots for the Al device. It is seen that for both Nb and Al devices,  $\sigma_s$  approximately follows the same function of  $\langle I_s \rangle$  by varying the bath temperatures or radiation powers: the distribution width has a plateau in higher switching current regime and then decreases with decreasing switching current monotonically<sup>25</sup>. In another word, one can obtain a certain switching current distribution  $P(I_s)$  by radiating the junction with a certain power at a fixed bath temperature, and the same  $P(I_s)$  (i.e., the same  $\sigma_s$  and  $\langle I_s \rangle$ ) can also be obtained with an un-irradiated junction by setting the bath temperature at a certain value. This suggests again that for the present devices, the optical responses of the switching current are mainly due to thermal effects and therefore the present junctions can be used as a desirable bolometer.

Principally, the weak light detection scheme in time domain is straightforward. One can bias the junction at a current slightly smaller than its switching current in the absence of radiation. If a light pulse with sufficient energy is applied, the switching current of the junction is reduced to below the bias current and then the junction will switch to a finite voltage state. Otherwise the junction will stay in zero voltage state. In this way one can judge if there are incoming photons or not.

Although the photon responsivity of the junction device demonstrated here is obviously lower than that of other superconducting detectors (such as the TESs and MKIDs), its performance in the weak light detection could be further improved by several methods. The first one is to enhance the coupling between the superconducting electrode of the junction and the incident photons. To this aim, one can use the lensed fibers to focus the light on the top electrode so that a maximum energy from the incident photons could be absorbed directly by the Cooper pairs on the electrode. Besides, the top metal electrode can be fabricated as thin as possible so that a certain radiation power can lead to a more reduction in the Cooper pair density. The second method to raise reponsivity is to reduce the thermal conductance between the chip and the sample holder to maximize the energy absorption by the whole chip. For instance, one can fabricate the junction on the substrate with low thermal conductivity (e.g., amorphous glass) or etch the back of the substrate wafer, to reduce the path of heat conduction from the chip to the sample block. By this way unnecessary radiation energy loss can be avoided effectively. The third method is to select materials with lower gap energies as the superconducting electrodes. Finally, for our experiments the fluctuations in the mean switching currents are limited by the low-frequency noises in the circuits, not by intrinsic noises of the junctions. Therefore, the device performance can be potentially improved by further re-

ducing the noise in the measurement electronics.

Besides the optical responsivity, there are two more challenges in our studied detection system. Firstly, the detection mechanism (i.e., by measuring the switching currents of Josephson junctions) can not be made very fast, since it takes time to sweep up the current and then sweep down to reset the junction to zero voltage state. The present measurement can be done at the rate up to several KHz, which is still a lower rate. By improving the bandwidth of the measurement electronics, the measurement rate can be faster but may not easy to get up to MHz. In addition, a faster measurement (i.e., a faster current ramping rate) will broaden the distribution width of the switching currents, which can decrease the detection sensitivity. Secondly, thermal activation is greatly suppressed at ultra-low bath temperatures, but the distribution of the switching currents still has a finite width  $\sigma_q$  due to quantum tunneling. For our tested Nb-junction sample and experimental parameters, one can calculate<sup>26</sup>  $\sigma_q = 101.87$  nA, which is very close to the observed distribution width  $\sigma_{s0}(Nb) = 102.73$  nA at  $T = 16$  mK, indicating the quantum tunneling is dominant at ultra-low bath temperatures. This finite distribution width may be translated to high dark counts for photon counting (as shown in Fig. 2, the blue and red curves have overlaps). However, this problem disappears when the junction device is only used as an optical power meter. One can statistically average the switching currents to distinguish the incident light powers. In the case of weak low-frequency circuit noise, the fluctuations in the average switching currents could be very small and thus the junction device can be utilized as a very sensitive radiation power meter.

In summary, we experimentally investigated the optical responses of the switching currents for the Al/AlOx/Al and the Nb/AlOx/Nb Josephson junctions at ultra-low temperatures ( $T \approx 16$  mK). The radiation power dependence of the relative switching current shifts were measured for both junctions. It was found that the Al-junction has a more sensitive optical response than the Nb-junction. The minimum radiation powers that the Al and Nb devices can respond to are about 8 pW and 2 nW respectively. Moreover, the Al-junction has been irradiated directly and indirectly through the substrate. It was observed that, the relative switching current shifts for both cases follows the same radiation power law dependence, indicating that the thermal effects are dominant in the optical responses. Hopefully, the junction devices demonstrated here can be applied to implement photon detections in the future, once the photon responsivity can be further improved.

This work was supported in part by the National Natural Science Foundation (Grant Nos. 61301031, 61371036, 11174373, 11204249), the Fundamental Research Funds for the Central Universities (Grant No. 2682014CX087) and the National Fundamental Research Program of China (Grant No. 2010CB923104). We thank Profs. Pei-

heng Wu, Xuedong Hu and Yang Yu for kind supports and valuable discussions.

- <sup>1</sup>G. N. Gol'tsman, O. Okunev, G. Chulkova, A. Lipatov, A. Semenov, K. Smirnov, B. Voronov, A. Dzardanov, C. Williams and R. Sobolewski, *App. Phys. Lett.* **79**, 705 (2001).
- <sup>2</sup>H. Kesue, S. W. Nm, Q. Zhng, R. H. Hdfield, T. Honjo, K. Tmki and Y. Ymmoto, *Nature Photonics* **1**, (343) 2007.
- <sup>3</sup>Aleksander D., Francesco M., David B., et al., *Nature Photonics* **2**, (302) 2008.
- <sup>4</sup>F. Marsili, V. B. Verma, J. A. Stern, S. Harrington, A. E. Lita, T. Gerrits, I. Vayshenker, B. Baek, M. D. Shaw, R. P. Mirin and S. W. Nam, *Nature Photonics* **7**, (210) 2013.
- <sup>5</sup>A. J. Miller, S. W. Nam, J. M. Martinis and A. V. Sergienko, *App. Phys. Lett.* **83**, 791 (2003).
- <sup>6</sup>L. Adriana E., A. J. Miller, and S. W. Nam, *Optics Express* **16**(5), 3032 (2008).
- <sup>7</sup>S. Friedrich, M. H. Carpenter, O. B. Drury, W. K. Warburton, J. Harris, J. Hall and R. Cantor, *J. Low Temp. Phys.* **167**, (741) 2012.
- <sup>8</sup>J. D. Teufel, Ph.D. Thesis, Yale University, 2008.
- <sup>9</sup>P. K. Day, H. G. LeDuc, B. A. Mazin, A. Vayonakis, and J. Zmuidzinas, *Nature(London)* **425**, 817 (2003).
- <sup>10</sup>J. Gao, M. R. Visser, M. O. Sandberg, F. C. S. da Silva, S. W. Nam, D. P. Pappas, D. S. Wisbey, E. C. Langman, S. R. Meeker, B. A. Mazin, H. G. Leduc, J. Zmuidzinas, and K. D. Irwin, *App. Phys. Lett.* **101**, 142602 (2012).
- <sup>11</sup>J. Gao, Ph.D. thesis, Caltech, 2008.
- <sup>12</sup>R. P. Feynman, B. L. Robert, and L. S. Matthew, *The Feynman Lectures on Physics*, Vol. **3**, Basic Books, 2011.
- <sup>13</sup>V. Ambegaokar and A. Baratoff, *Phys. Rev. Lett.* **10**, 486 (1963).
- <sup>14</sup>C. C. Grimes, P. L. Richards, and Sidney Shapiro, *J. App. Phys.* **39**(8), 3905 (1968).
- <sup>15</sup>D. P. Osterman, M. Radparvar, and S. M. Faris, *IEEE Trans. Magn.* **25**(2), 1319 (1989).
- <sup>16</sup>D. P. Osterman, P. Marr, H. Dang, C-T. Yao, and M. Radparvar, *IEEE Trans. Magn.* **27**(2), 2681 (1991).
- <sup>17</sup>M. S. Wire, L. O. Heflinger, B. J. Dalrymple, M. Leung, T. Pham, L. R. Eaton, and A. H. Silver, *IEEE Trans. App. Superconduct.* **3**(1), 2107 (1993).
- <sup>18</sup>E. Monticone, V. Lacquaniti, R. Steni, M. Rajteri, M. L. Rastello, L. Parlato, and G. Ammendola, *IEEE Trans. App. Superconduct.* **9**(2), 3866 (1999).
- <sup>19</sup>E. Monticone, M. Rajteri, R. Steni, M. L. Rastello, V. Lacquaniti, G. P. Pepe, L. Parlato, and G. Ammendola, *Int. J. Mod. Phys. B.* **13**(09n10), 1283 (1998).
- <sup>20</sup>M. Rajteri, E. Monticone, G. B. Picotto, R. Steni, M. Rastello, and V. Lacquaniti, in *Proceedings ICEC 17*, D. Dew-Hughes, R. G. Scurlock and J. H. P. Watson, Eds. Bristol and Phyladelphia: IOP Publishing, 711 (1998).
- <sup>21</sup>W. C. Stewart, *App. Phys. Lett.* **12**, 277 (1968).
- <sup>22</sup>T. A. Fulton and L. N. Dunkleberger, *Phys. Rev. B* **9**, 4760 (1974).
- <sup>23</sup>A. Barone, R. Cristiano, and P. Silvestrini, *J. App. Phys.* **58**, 3822 (1985).
- <sup>24</sup>G. Z. Sun, Y. W. Wang, J. Y. Cao, J. Chen, Z. M. Ji, L. Kang, W. W. Xu, Y. Yang, S. Y. Han, and P. H. Wu, *Phys. Rev. B* **77**, 104531 (2008).
- <sup>25</sup>H. F. Yu, X. B. Zhu, Z. H. Peng, Y. Tian, D. J. Cui, G. H. Chen, D. N. Zheng, X. N. Jing, L. Lu, and S. P. Zhao, *Phys. Rev. Lett.* **107**, 067004 (2011).
- <sup>26</sup>The theoretical distribution of switching currents due to quantum tunnelling is given by the equation:  $P(I_s) = \frac{\Gamma_q(I_s)}{dI/dt} \exp \left[ -\frac{1}{dI/dt} \int_0^{I_s} \Gamma_q(I) dI \right]$ , where  $dI/dt = 1.63 \times 10^{-2} A/s$  is the bias current ramp rate and  $\Gamma_q(I)$  is the well-known macroscopic quantum tunnelling (MQT) rate at bias current  $I$ . To calculate  $\Gamma_q$ , one needs to know the critical current  $I_c$  and shunt capacitance  $C$  of the Nb-junction. In our experiment, we obtain  $I_c = 126.66 \mu A$  by fitting to the average switching current and  $C = 0.26$  pF from independent microwave resonance experiment. The distribution width  $\sigma_q = 101.87$  nA can then be extracted once the distribution  $P(I_s)$  is obtained.